Supporting information:

The effects of inorganic additives on the nucleation and growth kinetics of calcium sulfate dihydrate crystals

Taher Rabizadeh[1*], Tomasz M. Stawski [1,2], David J. Morgan[3], Caroline L. Peacock[1], Liane G. Benning[1,2,4*]

1- Cohen Geochemistry Laboratory, School of Earth and Environment, University of Leeds, Leeds, LS2 9JT, United Kingdom

2- GFZ, German Research Centre for Geosciences, Telegrafenberg, 14473 Potsdam, Germany

3- Cardiff Catalysis Institute, School of Chemistry, Cardiff University, Cardiff, CF10 3AT, United Kingdom

4- Department of Earth Sciences, Free University of Berlin, 12249 Berlin, Germany

* Correspondence to: Taher Rabizadeh (eetr@leeds.ac.uk) and Liane G. Benning (Benning@gfz-potsdam.de)

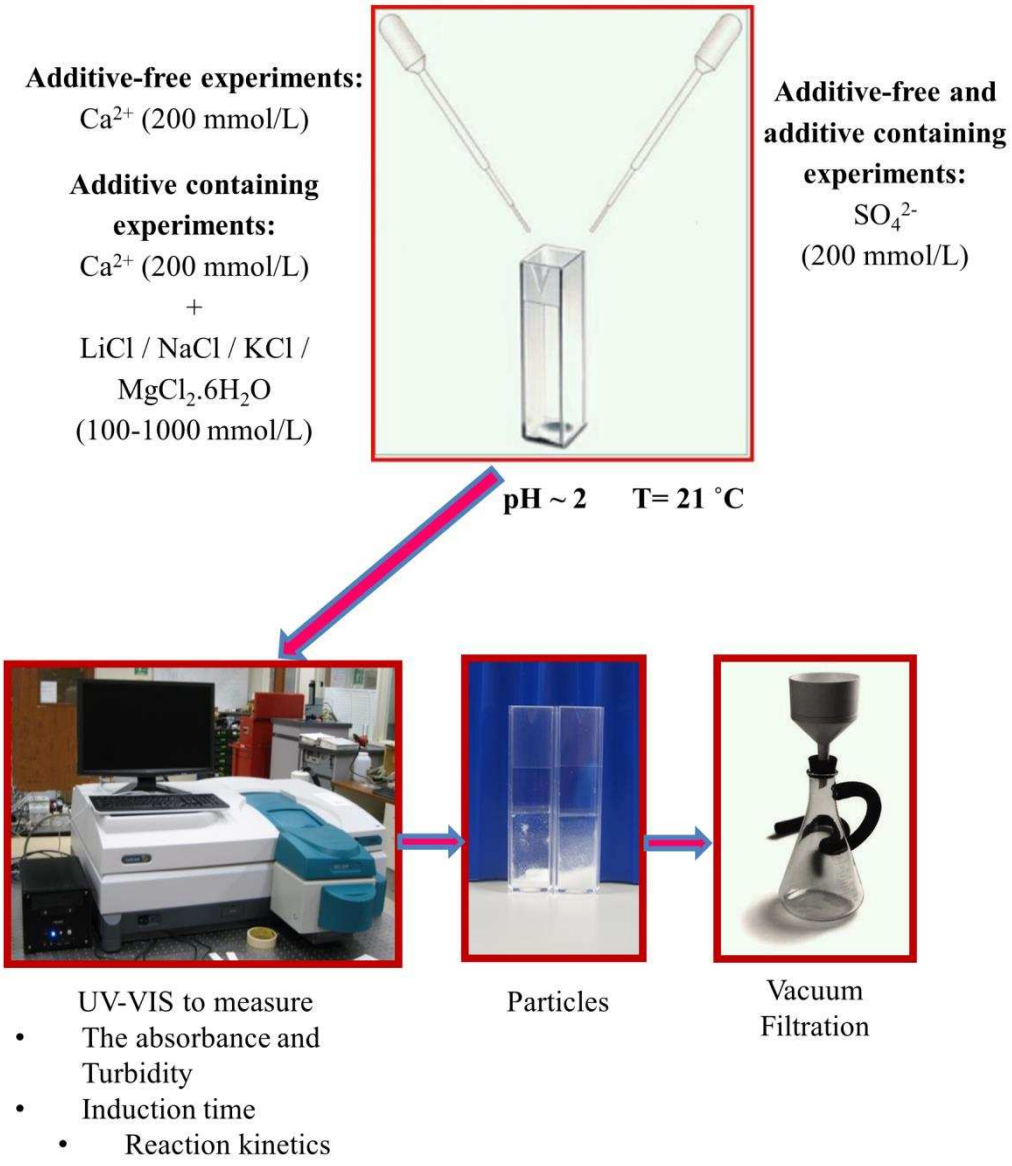

Figure S1. The schematic of producing calcium sulfate dihydrate in the presence and absence of additives.

Table S1. The limit of detection and uncertainty of ICP-MS / ICP-OES measurements.

	Li	Na	K	Mg	Ca
Limit of detection /ppm	3.35×10^{-4}	1.88×10^{-3}	4.07×10^{-3}	1.30×10^{-3}	4.50×10^{-3}
% uncertainty	1.62	2.02	2.08	1.38	2.09

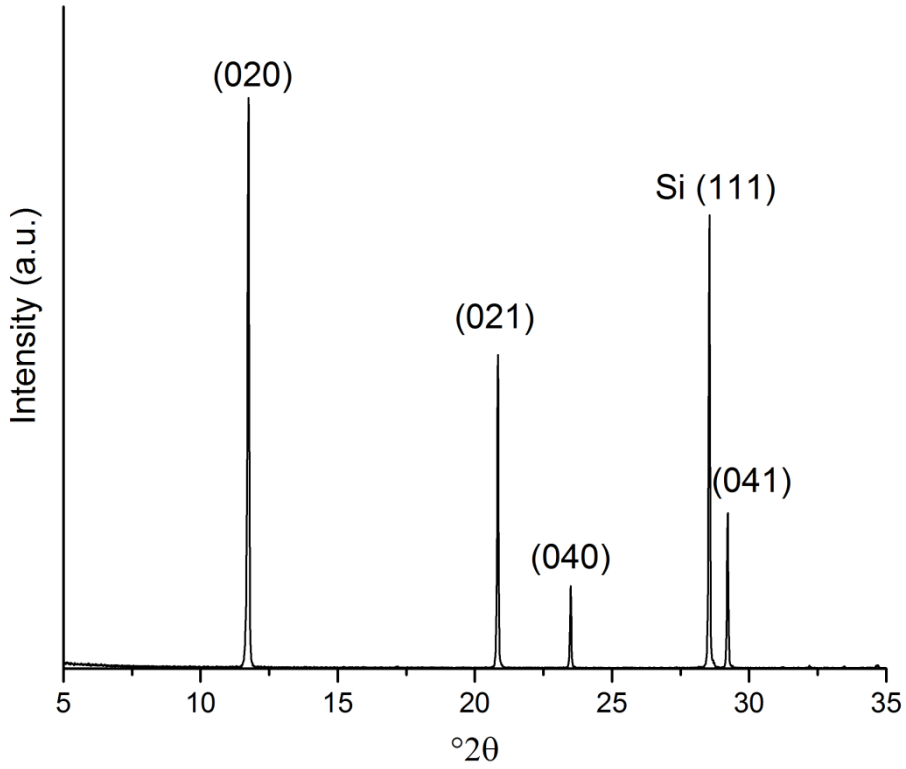

Figure S2. XRD pattern with marked Bragg peaks representative of crystals synthesized in the absence of additives confirming that the end-product was gypsum; Si (111) was used to determine the d-spacing precisely.

Table S2. Changes in induction time as a function of additive concentrations. Note that the induction time in the additive-free system was 3±1 minutes.

	Li^+			
concentration (mM)	50	100	300	500
induction time (min)	6±1	7±1	10±1	13±1
	Na^+			
concentration (mM)	50	100	300	500
induction time (min)	5±1	6±1	8±1	10±1
	K^+			
concentration (mM)	50	100	300	500
induction time (min)	5±1	6±1	7±1	8±1
	Mg^{2+}			
concentration (mM)	50	100	150	200
induction time (min)	9±1	17±1	23±3	32±4

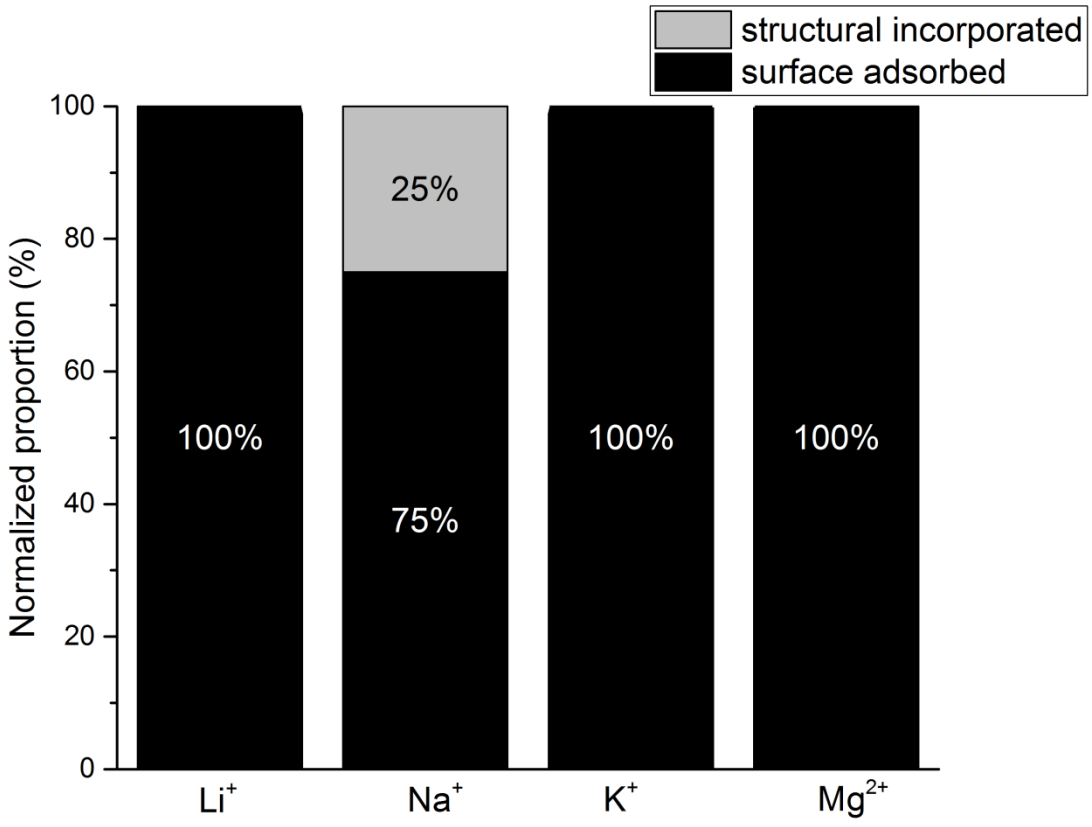

Figure S3. Partitioning of cations between gypsum crystal surfaces (adsorption) or crystal matrixes (structural incorporation).

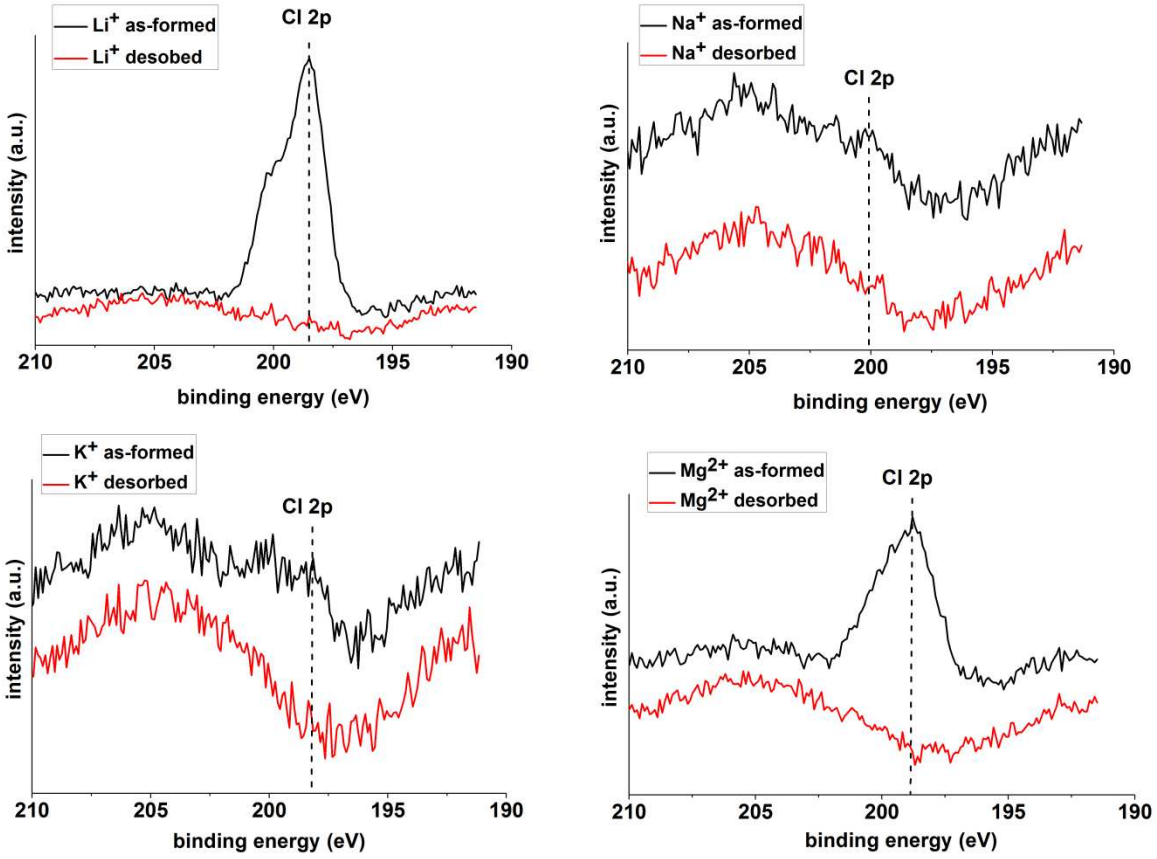

Figure S4. XPS spectra for Cl^- indicating that Cl^- was associated with the as-formed gypsum end-products (black patterns). Cl^- was removed during the desorption (red patterns) for all tested ions.

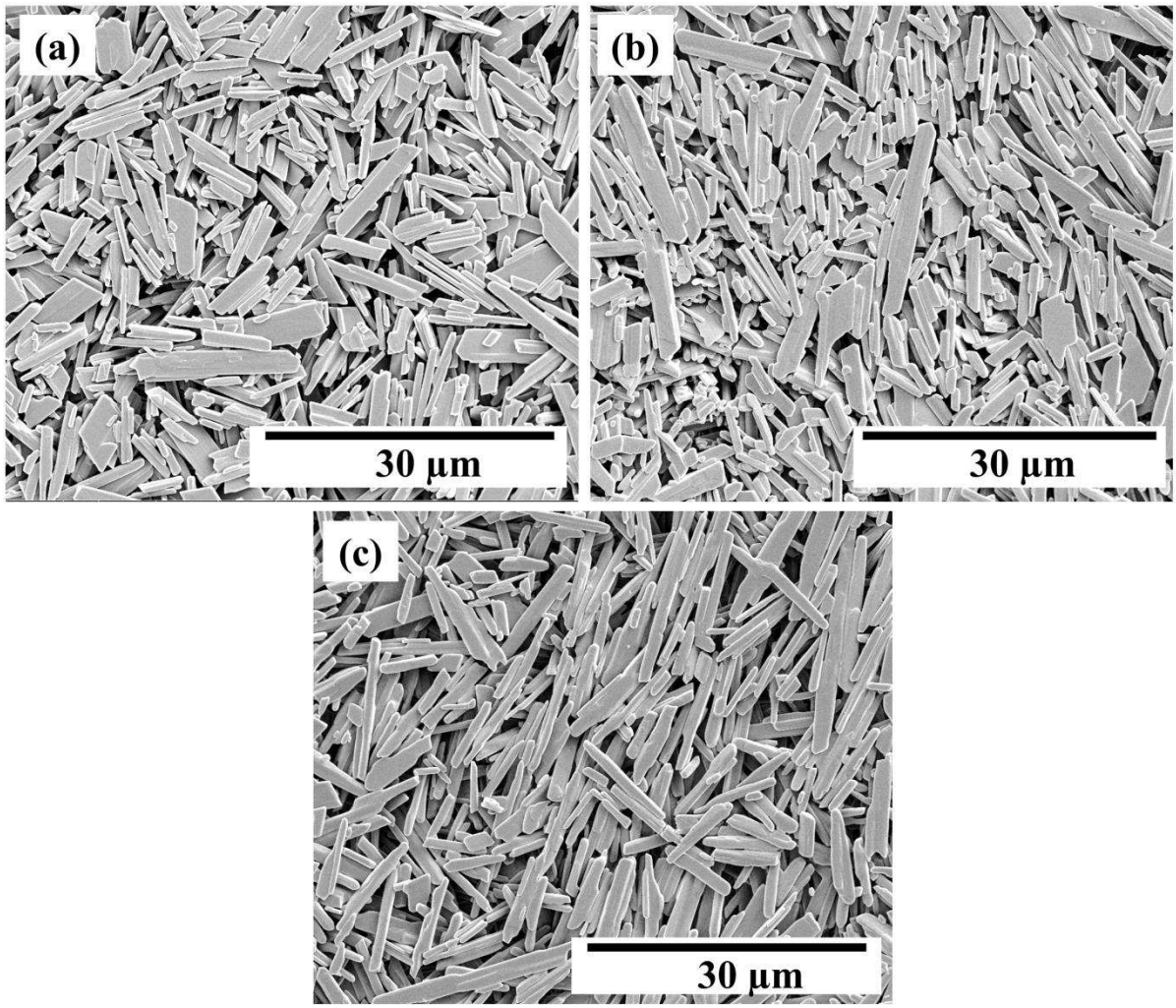

Figure S5. SEM morphology the gypsum crystals obtained after 200 min in the presence of (a) 500 mM Na^+ (b) 500 mM K^+ and (c) 200 mM Mg^{2+}.

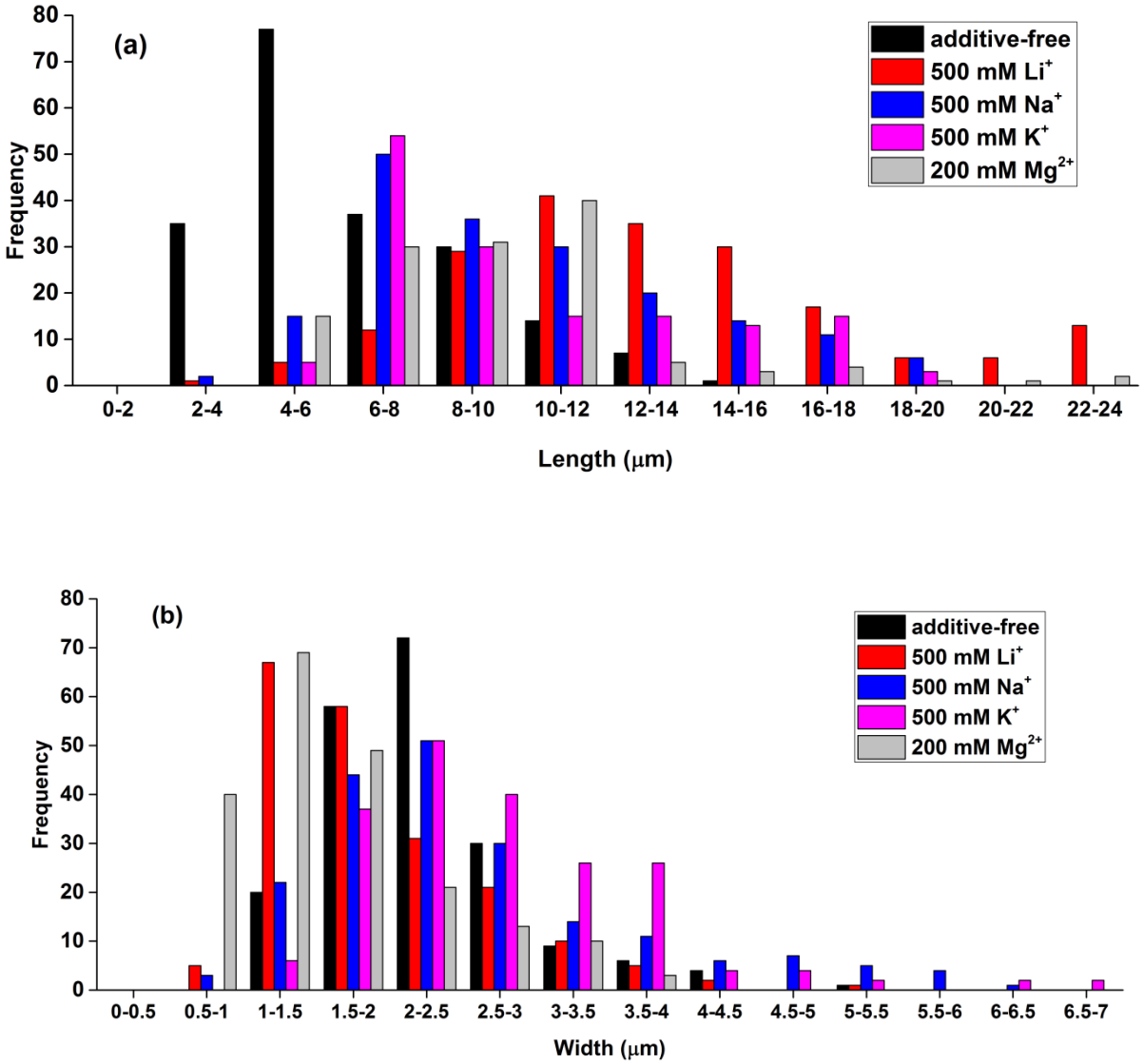

Figure S6. (a) Length and (b) width distribution of gypsum end-products precipitated in the presence and absence of additives.

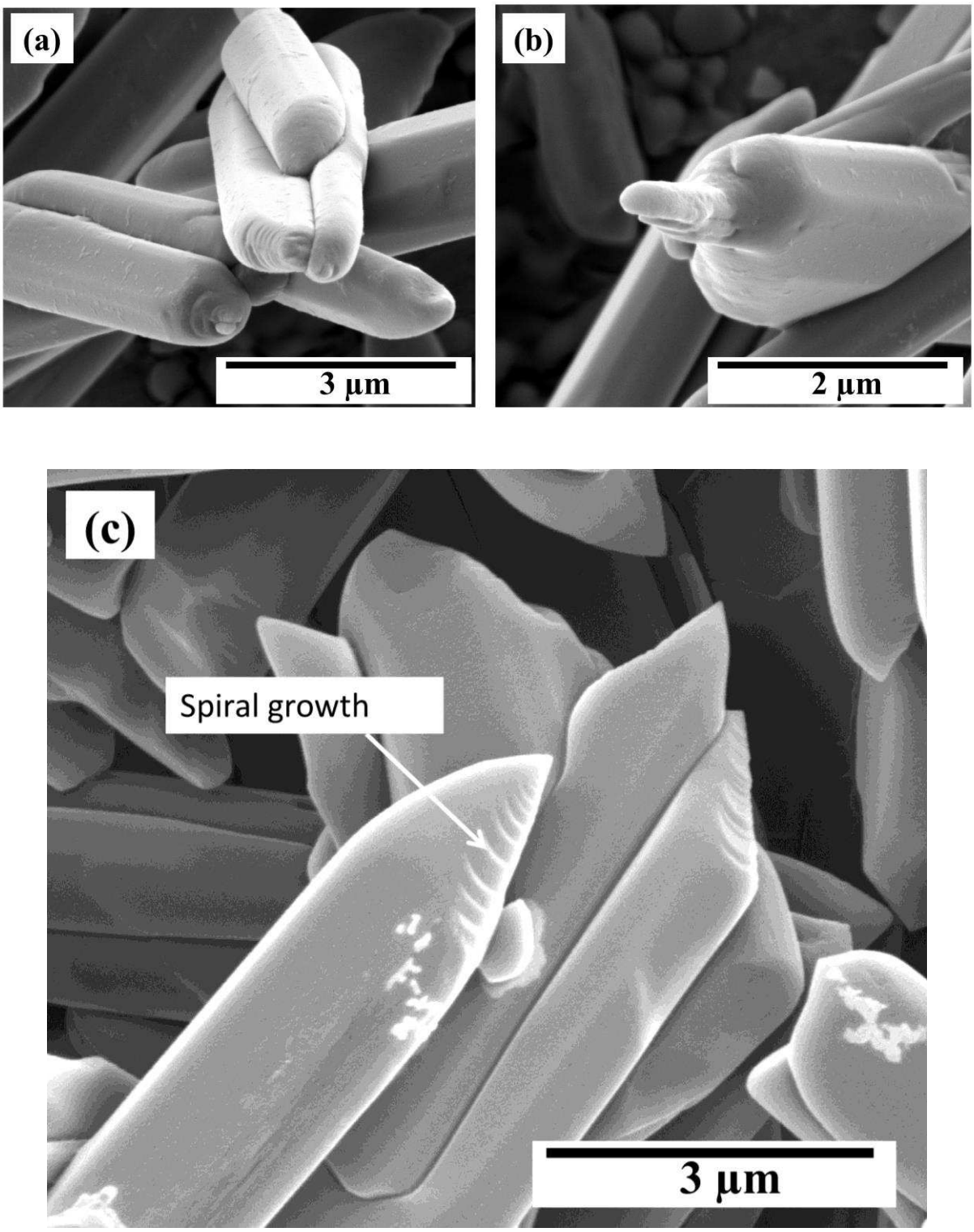

Figure S7. (a-c) SEM micrograph of gypsum crystals obtained after 200 min in the presence of 500 mM Li^+ illustrating the growth steps and the spiral growth mode visible at the crystals tips.

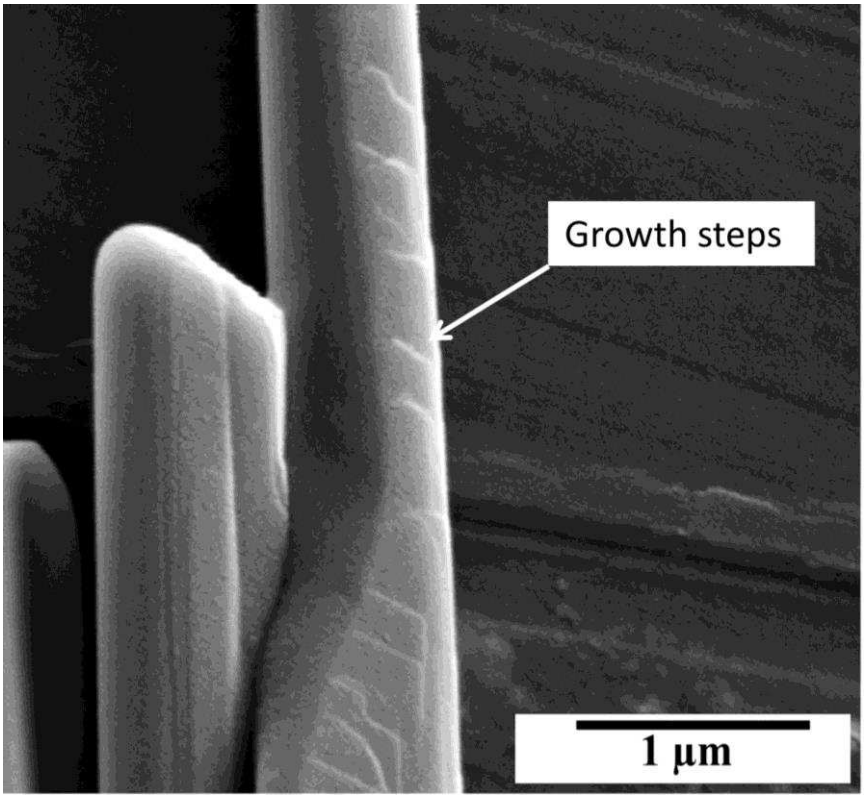

Figure S8. SEM micrograph of gypsum crystals obtained after 200 min in the presence of 500 mM Na^+ illustrating the uneven growth mode and growth steps.

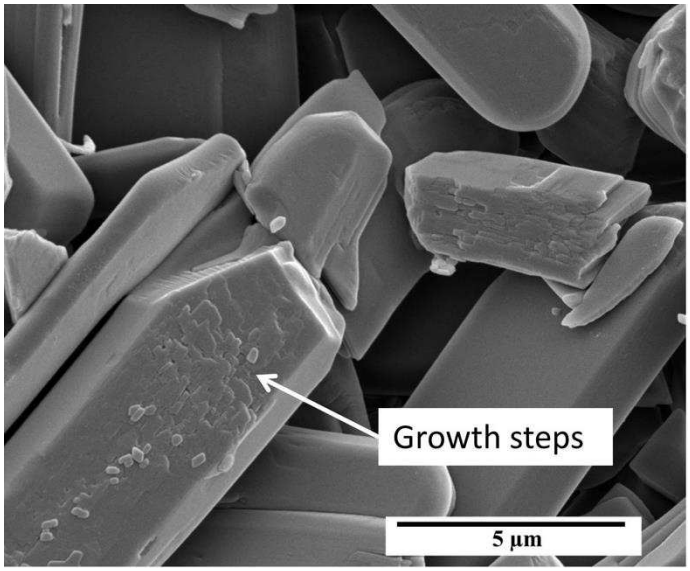

Figure S9. SEM micrograph from gypsum crystals obtained after 200 min in the presence of 500 mM K^+ illustrating the presence of growth steps.

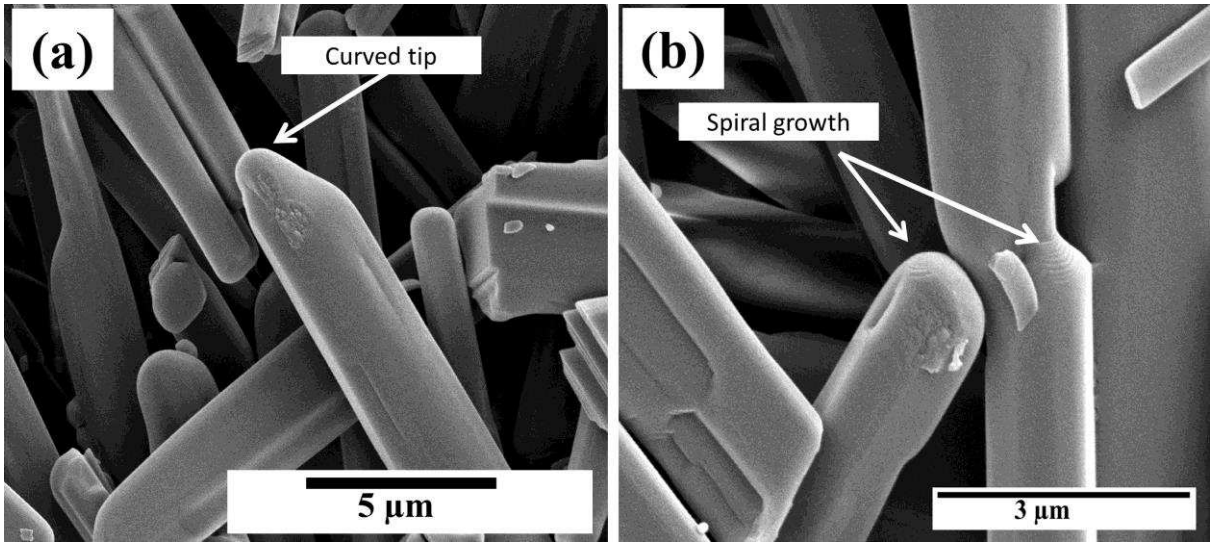

Figure S10. (a-b) SEM micrograph from gypsum crystals obtained after 200 min in the presence of 200 mM Mg^{2+} illustrating the presence of spiral growth and curved tips.

Table S3. Predicted saturation indices of gypsum crystals as a function of additive concentrations calculated by PhreeqC software. Note that the saturation index of gypsum in the additive-free system was 0.55.

	Li^+			
concentration (mM)	50	100	300	500
saturation index	0.53	0.51	0.43	0.37
	Na^+			
concentration (mM)	50	100	300	500
saturation index	0.53	0.51	0.43	0.38
	K^+			
concentration (mM)	50	100	300	500
saturation index	0.52	0.49	0.4	0.33
	Mg^{2+}			
concentration (mM)	50	100	150	200
saturation index	0.48	0.43	0.38	0.34

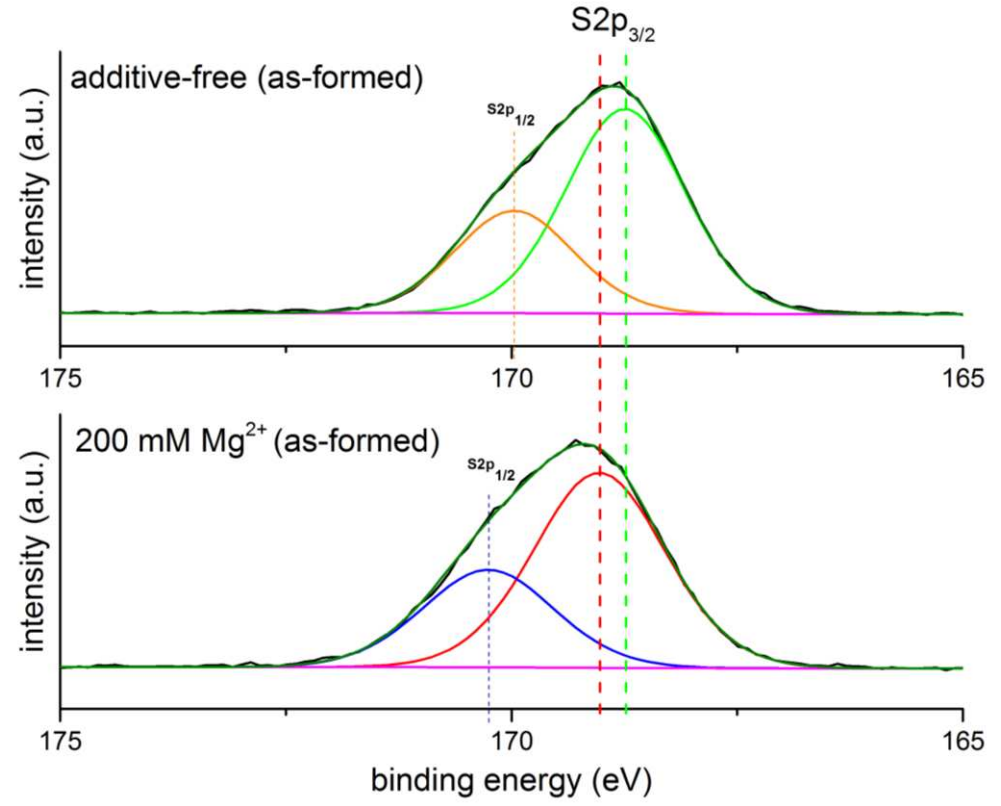

Figure S11. Mg^{2+} surface adsorption caused a 0.5 eV shift in $S2p_{3/2}$ binding energy towards higher binding energy.

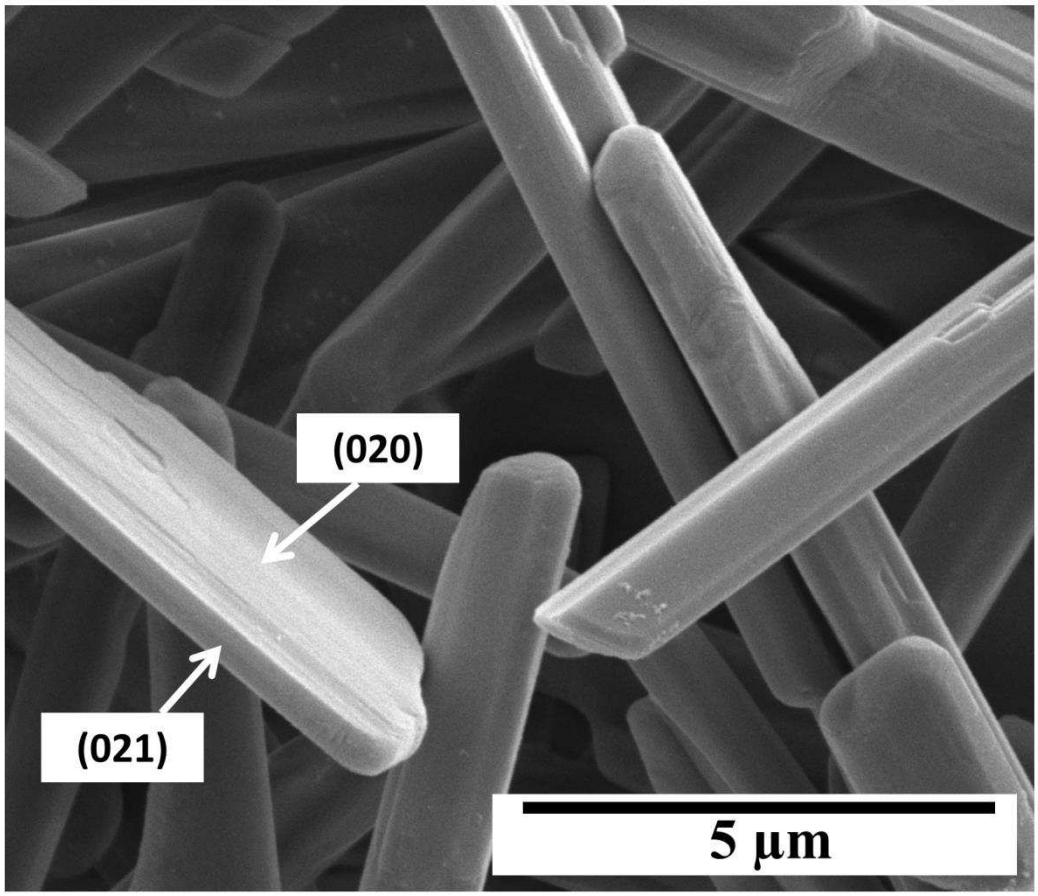

Figure S12. (020) and (021) faces of a gypsum crystal synthesized in the presence of 500 mM Na^+.